Role of thermal vibrations in molecular wire conduction

A. Pecchia, M. Gheorghe, A. Di Carlo, and P. Lugli
Dipartimento di Ingegneria Elettronica, Università degli Studi di Roma "Tor Vergata," via di Tor Vergata 110, I-00133 Roma, Italy

T. A. Niehaus and Th. Frauenheim
Department of Theoretical Physics, University of Paderborn, D-33098 Paderborn, Germany

R. Scholz
Institut für Physik, Technische Universität, D-09107 Chemnitz, Germany
(Received 30 May 2003; published 18 December 2003)

In the present work we investigate the influence of molecular vibrations on the tunneling of electrons through a molecule sandwiched between two metal contacts. The study is confined to the elastic scattering only, but beyond the harmonic approximation. The problem is tackled both from a classical and a quantum-mechanical point of view. The classical approach consists in the computation of the time-dependent current fluctuations along the step of a molecular-dynamics (MD) simulation. On the other hand, the vibrational modes are treated quantum mechanically and the tunneling current is computed as an ensemble average over the distribution of the atomic configurations obtained by a suitable approximation of the density matrix for the normal-mode oscillators. We show that the lattice fluctuations modify the electron transmission. However, the answers obtained with the two methods are different. At low temperatures, the quantum-mechanical treatment is necessary in order to correctly include the zero-point fluctuations. For temperatures higher than a few hundred kelvin the simple harmonic approximation which leads to the phonon modes breaks down because the oscillation amplitudes of the lowest-energy modes become very large. In this regime beyond the harmonic approximation, higher-order terms should be considered leading to phonon-phonon interactions and classical MD simulations prove to be simpler and give better results.

DOI: 10.1103/PhysRevB.68.235321 PACS number(s): 73.23.Ad, 73.63.Nm

I. INTRODUCTION

Recent developments in nanofabrication of molecular-scale devices renewed the attention of the scientific community on the properties of molecular entities and their potentiality as electronic components.[1–5] This type of technology can meet the demand of an increasing level of miniaturization and circuit density addressed by the information road map, and may provide a new class of ''intelligent'' electronic components for sensing applications in biological, medical, and industrial sectors. Understanding transport in such systems is a challenging problem. Heavy quantum-mechanical computations cannot be avoided in order to describe accurately the energy spectra and the exact nature of chemical bonding at the metal-molecule junctions, both crucial informations for quantitative predictions. Coherent tunneling versus activated,[6] phonon-mediated processes or redoxlike[7] mechanisms are still issues of debate and often the type of transport depends critically on the fabrication procedures and control of the interface quality.

One of the many aspects of molecular transport, which is relevant for molecular device electronics as well as scanning tunneling spectroscopy studies,[8] is a thorough investigation of the electron-phonon scattering, both elastic and inelastic. A number of works have been devoted to these subjects, including investigations of electron-phonon interactions in quantum wells,[9] molecular wires,[10] and tunneling through simple adsorbates on metal surfaces.[11–13] These works have been based on simple tight-binding Hamiltonians obtained from the linear expansion of the nondiagonal coupling terms or limited to simple model Hamiltonians in which the electrons are coupled to a small number of vibrational modes.

Ab initio quantum-mechanical treatments of the electron-phonon coupling in such systems may be a very hard computational task, since the basis set required for the description of the electron and phonon degrees of freedom becomes overwhelmingly large already for small molecules. For instance, in a molecule comprising 20 atoms, and consequently 60 vibrational modes, even after a restriction of the Fock space to the values of 0 or 1 for the possible phonon occupations in each mode, the basis size will have the dimension of $2^{60} \approx 10^{18}$. However, larger basis sets must be used in general in order to obtain converged results. Of course a large number of the vibrational modes may be neglected because they have small electron-phonon coupling; nonetheless, a brute force computation for realistic systems may turn out to be impractical.

The advantage of solving the problem as a direct diagonalization in Fock space is that afterwards it is possible to clearly separate the inelastic tunneling channels from the elastic ones.[14–17] The inelastic tunneling involves emission or absorption of one or more phonons. The elastic component is given essentially by the interference between the transmission in perfect equilibrium conditions (in the absence of vibrations) and paths which involve creation-annihilation processes of virtual phonons. This approach contains a number of strong approximations, originating mainly from the harmonic approximation, the normal-mode decoupling, and the entire treatment of the electron-phonon coupling. Under these assumptions, the influence of molecu-

lar vibrations on the electronic tunneling is a small correction to the ideal tunneling obtained for the equilibrium configuration. Moreover, even a small molecule can have soft vibrational modes, resulting in large oscillation amplitudes already at low temperatures. Therefore, the usual approximation to the electron-phonon coupling is not valid and the elastic component of the tunneling is better represented by the average of the elastic tunneling over a set of deformed configurations of the molecule. In this paper we study the influence of molecular vibrations on the tunneling current in molecular electronic devices. We consider a simple model system represented by a *di-thio-phenylene* molecule sandwiched in between two gold contacts via sulfur bonds. The transport is dominated by charge-carrier tunneling inside the gap between the highest occupied molecular orbital (HOMO) and the lowest unoccupied molecular orbital (LUMO). This gap, along with the Fermi energy alignment, is a crucial parameter for controlling the conductance of a molecule, because the transmission increases with a decreasing gap, corresponding to smaller barriers for tunneling. The gap of the molecule depends on the chemical nature and the atomic structure of the system. It can be modified by the electron-electron interactions, thermal lattice fluctuations, or electron-lattice interactions. The calculations highlight the importance of the position of the molecular electronic levels with respect to the Fermi levels of the contacts in the presence of an applied voltage. This numerical approach is based on a combination of scattering and Green's-function theory with a tight-binding treatment of the density-functional Hamiltonian. This model allows for a self-consistent treatment of the quantum transport across a molecular system connected to two semi-infinite leads.

A molecular-dynamics (MD) simulation is performed in order to give a classical approximation to the molecular vibrational trajectory. For subsequent time steps of the MD simulation we compute the instantaneous tunneling probability and related current intensity through the molecule. The time-averaged current obtained using the MD simulation has been compared with the ensemble average over the molecular configurations, obtained by a quantum-mechanical treatment of the vibrational modes. The average is performed by a random Monte Carlo sampling of the atomic configurational space. This comparison shows that the harmonic approximation and the linear approximation for the electron-phonon coupling can lead to inaccuracies already at relatively small temperatures.

The paper is structured as follows. In Sec. II we briefly review the quantum theory of the molecular vibrations and the theory of electron transport through organic molecules whose ends are connected to conducting leads. In the Sec. III the result of our computations are presented. In Sec. III A the frequency spectrum of a di-phenylene molecule is computed and compared to other methods and experimental results. The effect of lattice fluctuations on the tunneling current through a di-thio-phenylene molecule is then discussed in Sec. II B. A similar discussion is also extended to a prototypical molecule proposed as an electronic rectifier in Sec. III C. Finally, in Sec. IV, the time-dependent current computed with the MD simulations is analyzed in its frequency components. The latter spectrum is compared to the frequencies of the eigenmodes.

II. THEORETICAL MODEL

A. Intramolecular vibrations

The Born-Oppenheimer approximation consists of a separation of the nuclear and the electronic degrees of freedom by assuming that the electrons can adapt instantaneously to the nuclear positions. The electronic part is solved for each frozen nuclear configuration to yield an effective potential in which the nuclei move. The standard textbook procedure for the study of the nuclear motion is to expand this effective potential up to the harmonic term, and to decouple the Hamiltonian as a superposition of independent one-dimensional oscillators which correspond to the different vibrational eigenfrequencies,

$$H=\sum_{q=1}^{3N}\left(-\frac{\hbar^2}{2m_q}\frac{\partial^2}{\partial\xi_q^2}+\frac{m_q}{2}\omega_q^2\xi_q^2\right), \tag{1}$$

where N is the number of atoms, m_q the reduced mass of the mode q, and ω_q the mode frequency. The quantities ξ_q represent the displacements along the directions corresponding to the mode eigenvectors $\mathbf{e}^q$. Each independent harmonic oscillator can be treated quantum mechanically, giving the well-known spectrum of discrete energy eigenstates, $E_n=\hbar\omega_q(n+1/2)$. In the language of second quantization, n can be viewed as the number of phonon quanta occupying the mode and having an energy $\hbar\omega_q$. According to statistical mechanics, for each harmonic oscillator in thermodynamical equilibrium with a thermal bath of temperature T, it is possible to derive the following form for the normalized distribution over the deformations ξ_q:[18]

$$P_q(\xi_q)=\sqrt{\frac{m_q\omega_q^2}{2\pi E_q^{th}}}\exp\left(-\frac{m_q\omega_q^2\xi_q^2}{2E_q^{th}}\right). \tag{2}$$

Here E_q^{th} is the thermal energy of the mode q, expressed by

$$E_q^{th}=\left[n_q^{th}+\frac{1}{2}\right]\hbar\omega_q, \tag{3}$$

where n_{th} is the average number of excited quanta in the oscillator, given by the usual Bose-Einstein distribution. This form of the density gives the expected averages for the kinetic and potential energies and respects Virial's theorem, $U=K=E_{th}/2$. The atomic displacements from the equilibrium configuration are given by a superposition of the displacements along the modes,

$$\Delta\mathbf{r}=\sum_{q=1}^{3N}\xi_q\mathbf{e}^q, \tag{4}$$

and the distribution over deformed molecular configurations can be obtained as a product of the independent distributions for each mode,

$$P(\{\xi_q\}) = \prod_q P_q(\xi_q, E_q^{th}). \tag{5}$$

This distribution can be used for the computation of the quantum-mechanical averages over the ensemble of the atomic configurations. It will be used in the following to compute the average transmission probability across a molecule including the atomic coordinate fluctuations around equilibrium. In the Boltzmann limit, the thermal energy in Eq. (3) should be replaced by kT. Inserting this value in Eq. (2) the well-known Boltzmann distribution $P \approx \exp(-V/kT)$ is recovered.

B. The tunneling current in molecular systems

In this section the basic elements used for the computation of the tunneling current across a molecule are described. We are interested in modeling the coherent electron transport through a finite-size system connected to two leads injecting or collecting the charge carriers. The system is described via a density- functional tight-binding Hamiltonian (DFTB).[19,20] This method uses a minimal, but optimized, basis set. This is usually sufficient for the first and second row elements, whereas the sulfur element is treated with a polarized basis including the unoccupied *d* orbitals. In order to compute the current flowing across the molecule, open boundary conditions for the Kohn-Sham equations must be employed, otherwise the eigenstates do not carry any current. Usually, the current is computed in the context of scattering theory,[21] transfer matrix,[22] or via Green's-function techniques.[23,24] Beside the numerical stability, Green's-functions technique has the advantage that scattering, decoherence, and energy relaxation can be treated in a unified formalism. The problem of quantum transport through a mesoscopic device linked to two contacting leads is essentially a nonequilibrium problem. Deep in the contacts the propagating states are kept in equilibrium with the thermal bath via dissipative scattering events, but the device region is kept out of equilibrium by the applied bias. In small molecular systems and for large biases, the current is dominated by tunneling and the energy relaxation occurs at the collecting electrode. The starting point is the determination of the density of states and the electronic density in the device region, knowing the boundary conditions imposed by the transport problem. In this case, the problem of transport cannot be separated from the computation of the density of states, because the states themselves are scattering states carrying a net current. In the density-functional approach, the electronic density is the essential ingredient for the computation of the Hamiltonian which determines, in turn, the scattering states. Therefore, a self-consistent computation of the states and the current should be carried out.[25] The retarded (advanced) Green's function of the system can be expressed as

$$G_M^{r(a)} = [(E \pm i\delta)S_M - H_M - \Sigma^{r(a)}]^{-1}, \tag{6}$$

where H_M and S_M are the Hamiltonian and overlap matrices of the molecular system and $\Sigma^{r(a)}$ is the sum of the self-energies due to the interactions with the contacts. This is given by

$$\Sigma^{r(a)} = \sum_\alpha [ES_{M\alpha} - T_{M\alpha}] g_\alpha^{r(a)} [ES_{M\alpha} - T_{M\alpha}]^\dagger, \tag{7}$$

where $T_{M\alpha}$ is the Hamiltonian between the molecule and the contact α. In the general case, the self-energy includes, besides the contact self-energy,[26] terms corresponding to scattering events resulting from electron-phonon or electron-electron interaction. The self-energy due to the phase-breaking interactions can be expressed, in many-body perturbation theory, via the Dyson's equation in terms of Green's function itself. This self-energy contains an imaginary part which plays the role of reshuffling electrons between different energy channels. In the limit in which incoherent scattering is absent, the elastic transmission through the molecule is given by[27]

$$T(E) = \mathrm{Tr}[\Gamma_2 G^r \Gamma_1 G^a], \tag{8}$$

where $\Gamma_{1,2}$ represent the imaginary parts of the self-energy of contact 1 and 2, respectively. The tunneling current can be expressed as

$$i_{coh} = \frac{2e}{h} \int_{-\infty}^{+\infty} T(E)[f_2(E) - f_1(E)]dE \tag{9}$$

corresponding essentially to the expression derived in Landauer theory.

In order to speed up the computations we approximate the contact Green's functions as diagonal matrices with imaginary elements given by the local density of states of a bulk metal. This approximation is valid in the limit in which the coupling of the molecule to the *k* states of the bulk contact is not strongly *k* dependent. It can be justified on the basis of the following approximation:

$$\Sigma^r = \sum_k T_{Mk} \frac{1}{E - E_k} T_{kM}^\dagger \approx -i\pi \langle |T|^2 \rangle \rho(E), \tag{10}$$

where the real part of Σ has been neglected. The coupling term is approximated by the coupling of the S atom of the molecule with a gold atom of the contact. It is well known that the s-wave approximation does not lead to correct results for π-conjugated molecules, because both the HOMO and LUMO are π orbitals which cannot couple to *s* orbitals because of their symmetry. In order to solve this problem, we have modeled the Au atoms with an sp^3 basis set. The π symmetry arises in the usual geometry in which the thiolates bind to the Au surfaces, corresponding to a Sulfur atom binding to a hollow site of the Au(111) surface.[28] The Au density of states is fixed to the value at the Fermi energy $\rho(E_f) \approx 0.07\ \mathrm{eV}^{-1}$ and the relevant S-Au π-π coupling Hamiltonian has an average value of about 6.8 eV.

C. Elastic transmission through the quantum phonon field

The elastic transmission through the vibrating molecule can be computed using an adiabatic approximation, in which the transmission is obtained as an average over the instantaneous transmissions computed for each frozen molecular configuration. In principle, this average should be taken over the ensemble of all the possible configurations of the mol-

ecule, weighted by the distribution in Eq. (5). Therefore, the average transmission can be obtained by an integration over the configuration space

$$\langle T(E)\rangle = \int d\xi_1 \xi_2 \cdots d\xi_{3N} T(E;\{\xi_q\}) P(\{\xi_q\}). \quad (11)$$

As this integration has to be evaluated in a $3N$-dim space, the best suited method is a Monte Carlo (MC) technique sampling the configuration space randomly with weights according to $P(\xi_q)$. For a set of random coordinates ξ_q the deformation of the molecule is given by Eqs. (2) and (4). For each of these configurations, the Hamiltonian and overlap matrices can be recomputed. From these ingredients the transmission $T(E)$ of Eq. (8) can be calculated from the molecular Green's function of Eq. (6), obtained with direct numerical inversions.

Finally, using Eq. (9), the current is computed from the average transmission. However, particular care is needed in the computation of the average using the Monte Carlo method. It is known[29] that the ensemble average of the transmission probability in a disordered one-dimensional conductor is a statistically ill-defined quantity because it is dominated by a very small number of exceptional configurations. In other words, the average is in no way representative of the typical transmission probability to be expected from a randomly sampled member of the ensemble. This difficulty does not arise if $\ln T(E)$ is averaged instead of $T(E)$.[30] Therefore, the procedure we have followed was to compute the average tunneling as $\langle T(E)\rangle = \exp(\langle \ln[T(E)]\rangle)$. For each temperature, the phonon fluctuations are averaged over 500 random configurations. The convergence of this sampling procedure was checked by doubling the size of this ensemble, resulting in no significant changes of the average transmission.

D. Molecular-dynamics treatment of the vibrations

The quantum-mechanical treatment of the vibrational modes has been compared to a time average obtained by classical MD simulations. In this approach the molecular configurations follow the dynamics of the molecule. The time evolution is obtained with a Verlet algorithm[31] with a random rescaling of the atomic velocities in order to thermalize the kinetic energy to the value of $3Nk_BT/2$ for N atoms involved.[32] This limiting value is in agreement with the classical energy of $3N$ harmonic oscillators and coincides with the high-temperature limit of the quantum-mechanical treatment. Therefore, assuming that the system is ergodic, we would expect that the average transmission obtained with the MD simulations corresponds essentially to the same result of the quantum-mechanical average in the limit of high temperatures. The MD simulations were carried out for a time interval of about 11.5 ps of time, corresponding to about 120 000 time steps of 4 a.u.$=0.096$ fs. Like the quantum case described above, the average transmission is calculated over the transmission computed for successive molecular configurations. As the most time consuming part of the algorithm is the computation of Green's function, this calculation was performed every 40th time step of the MD simulation, resulting in 3000 sampling times.

TABLE I. Results of the computation for the normal modes for DPA. The table shows the comparisons between the DFTB computation and measured values. In braces are reported theoretical results using the semiempirical PM3 method. Frequencies are expressed in cm^{-1}.

Mode	Symmetry	DFTB	Expt/(PM3)[a]
1	A_u	16.44	(35)
2	B_{3g}	38.04	(51)
3	B_{2u}	45.67	(52)
4	B_{2g}	118.92	147
5	B_{3g}	102.43	174
6	B_{3u}	270.02	280
7	A_g	274.91	261
8	B_{1g}	377.93	407
9	A_u	378.49	(358)
10	B_{2g}	327.49	388
11	B_{2u}	471.63	467
12	B_{3u}	492.52	509
⋮	⋮	⋮	⋮
64	B_{2u}	3059.94	3069
65	B_{1u}	3063.80	3078
66	A_g	3064.05	3084

[a]From Reference 31.

III. RESULTS

A. Vibrational spectrum of di-phenyl-acetylene

In this section we compare the frequency spectrum calculated with the DFTB code to the results of semiempirical methods and available experimental data. These test calculations are performed for the vibrational spectrum of di-phenyl-acetylene (DPA), resembling the di-thio-phenylene molecule used in the following sections for the calculation of the tunneling current between two Au contacts. Even though the low-frequency vibrations are difficult to access experimentally these are precisely the modes with strong influence of the zero-point fluctuations on the tunneling current. Most of the time these modes are optically inactive or very weakly active because of symmetry or because they involve oscillations of large molecular portion with very small dipolar coupling. However, these modes can be very relevant for electronic transport properties, because they can have the effect of breaking the coherent tunneling path. For example, in the DPA the twist oscillations of the phenyl rings around the central triple bond strongly affect the conjugation between the two rings and the tunneling across the molecule.[33] The result of our computations are reported in Table I. The table shows the lowest-energy modes of DPA as computed with DFTB compared to the experimental results taken from Ref. 34. Whenever the experimental result was not available we have reported the theoretical values obtained with the semiempirical method PM3.[34]

Recently, the DFTB method has been recently applied successfully to study the vibrational frequencies of perylene tetracarboxylic dianhydride (PTCDA),[35,36] and also in the present case it compares relatively well. In the following, it is important to observe that DFTB tends to underestimate the

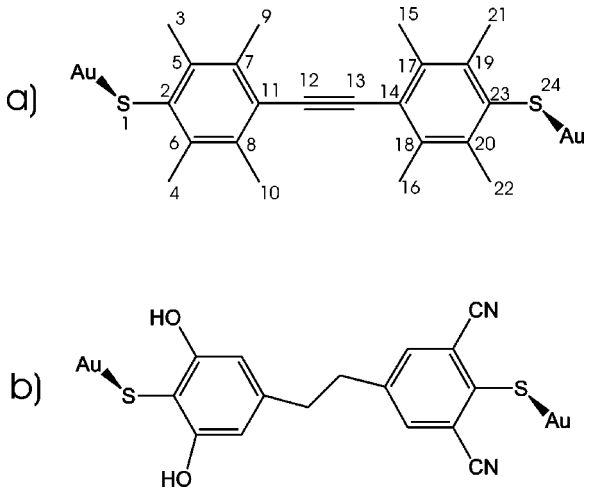

FIG. 1. Representation of (a) di-thio-tolane and (b) dihydroxy-dicyano-diphenylene molecule between two Au contacts.

mode frequencies of the torsional modes, although the relative error decreases considerably as the frequencies increase. The lowest mode corresponds to the twist of the two phenyl ring around the principal axis of the molecule. It is difficult to obtain an accurate frequency for this mode by direct diagonalization of the numerically computed Hessian, despite the fact that the molecular geometry was relaxed to the level at which the atomic forces were lower than 5×10^{-6} a.u. These problems arise from the computation of the Hessian out of the total energy for slightly deformed geometries around the global minimum: large deformations would reduce the influence of numerical fluctuations arising in the diagonalization, a requirement which has to be optimized against the validity range of the harmonic approximation.

B. The effect of lattice fluctuations on the tunneling current

We have investigated the influence of vibrations on the transmission across a molecule of di-thio-tolane (DTT) and a dihydroxy-dicyano-diphenylene rectifying molecule (DDP). The molecules are connected to the contacts via covalent Au-S bonds, as shown in Fig. 1. In the computation of the molecular vibrations, the Au atoms of the contacts are kept fixed. This can be considered as a reasonable approximation given the relatively large mass of the Au atoms with respect to the C and H atoms forming the molecule. First we discuss the results obtained for the DTT molecule. After the relaxation of the atomic coordinates, obtained by imposing the atomic forces to be smaller than 10^{-4} a.u., the molecule was found on a planar geometry. The vibrational frequencies together with a description of the modes are reported in Table II. Since the molecule is constrained by the fixed contacts, the rotational and translational invariance is broken and therefore the six corresponding improper modes are absent. The system comprises 72 proper modes of vibrations. The lowest vibrational mode, with a frequency of only 8 cm^{-1}, corresponds to a molecular oscillation in the plane of the phenyl rings resembling the first harmonics of a string with the two sulfur atoms remaining fixed. The second mode is similar, with the exception that it corresponds to a vibration perpendicular to the phenyl plane. The third mode is the rigid twist of the two phenyl rings around the central triple bond. The fourth and sixth modes can be described as a second harmonic of a vibrating string, with a node in the center of the molecule. The higher modes correspond to a rigid motion of the phenyl rings with predominant shear oscillations of the triple bond. In mode 7 the parallel bend of the rings is accompanied by an oscillation of the whole molecule along the z direction. The Au-S stretch frequency is around 390 cm^{-1}, whereas above 600 cm^{-1} the internal vibrational modes of the DPA are recovered.

TABLE II. Vibrational frequencies and mode description for the DTT molecule.

Mode	Frequency (cm^{-1})	Mode description
1	8.00	$\parallel$ string vibration
2	12.17	$\perp$ string vibration
3	20.58	Ph twist
4	46.32	$\perp$ string vibration (II harm)
5	75.60	C-Ph $\perp$ bend (boat)
6	83.79	$\parallel$ string vibration (II harm)
7	86.78	C-Ph $\parallel$ bend and z oscillation
8	97.15	C-Ph $\perp$ rotation
9	151.12	$\perp$ bend (III harm)
10	178.04	C-Ph $\parallel$ rotation S z oscillation
⋮	⋮	⋮
70	3058.66	C-H Stretch
71	3061.26	C-H Stretch
72	3061.62	C-H Stretch

The spectral transmissions for different temperatures are shown in Fig. 2, for the energy window between -7.0 eV and -1.4 eV, covering the HOMO-LUMO gap. In this scale, the Au Fermi energy is located at -4.25 eV. Figure 2(a) refers to the MD simulations and Fig. 2(b) to the quantum Monte Carlo average. These two computational schemes give different results even in the limit of high temperatures. At a temperature of 10 K, the transmission function obtained with the MD simulation coincides essentially with the one obtained for the molecule in equilibrium presenting sharp features in correspondence to the HOMO and LUMO bands. In the quantum-mechanical counterpart, the same features are broadened already at 10 K because of the zero-point motion of the internal vibrations.

Increasing the temperature from 10 K to 50 K, the transmission inside the gap increases, whereas the transmission resonances tend to decrease both in the MD simulations and in the quantum MC computations. This is due to the fact that the molecular vibrations induce fluctuations in the HOMO-LUMO gap. Since the transmission inside the gap depends,

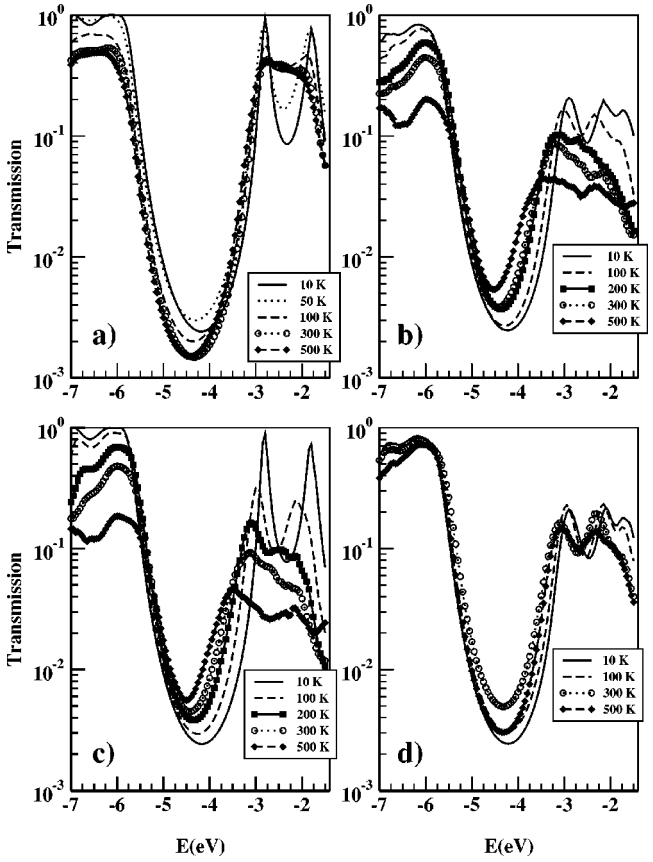

FIG. 2. Transmission functions of DTT as a function of temperature obtained from (a) the MD simulations; (b) the MC with quantum oscillators; (c) the MC with classical oscillators; and (d) the MC with quantum oscillators with frequencies shifted up by 20 cm^{-1}. The Fermi level of the Au metal is at -4.25 eV.

to first order, on the inverse of the energy difference between the HOMO (LUMO) and the injection energy, the current is enhanced because, on average, the gap reduction dominates. On the contrary, the injection at the LUMO or HOMO energies decreases on average, because the same fluctuations bring the levels in and out of resonance, where the transmission is almost unitary.

The typical deviations from the average are shown in Fig. 3, where the transmission for different configurations are visualized for the MD simulation [Fig. 3(a)] and for the quantum-MC [Fig. 3(b)]. Both computations were obtained for a temperature of 50 K, giving clear evidence for larger deviations in the quantum-mechanical ensemble. At a temperature of 100 K and above, the average transmission obtained with the MD simulations starts to decrease, both inside the gap and at resonance. On the other hand, in the quantum MC the behavior is qualitatively different since the transmission progressively increases further inside the gap and decreases at resonance. This indicates that the simple harmonic approximation comes to the limits of its validity. Two separate effects contribute to this result. First, above 100 K, the thermal energy is sufficient to overcome the low-energy barrier for the phenyl rotations around the triple bonds (9.5 meV). As the molecule begins to rotate the average transmission decreases, because the transmission for the configuration in which the phenyl rings are perpendicular to each other is very small.[33] The other very important problem arising in the quantum computations is that the oscillation amplitude increases with temperature beyond the validity range of the normal-mode analysis. This effect can be seen in Fig. 4, which represents the potential profile corresponding to the twist mode of the phenyl rings in the DPA molecule. The atomic displacements along the mode eigenvectors is accompanied by a relevant stretching of the rings [Fig. 4(a)] with a potential profile deviating from the harmonic approximation already for very small amplitudes. For comparison, the potential barrier for rotation of one ring with respect to the other is shown in Fig. 4(b).

The standard deviation of the atomic displacements as a function of temperature is visualized in Fig. 5 for the six lowest internal vibrational modes. The atomic index in the abscissa refers to numbering reported in Fig. 1. The middle

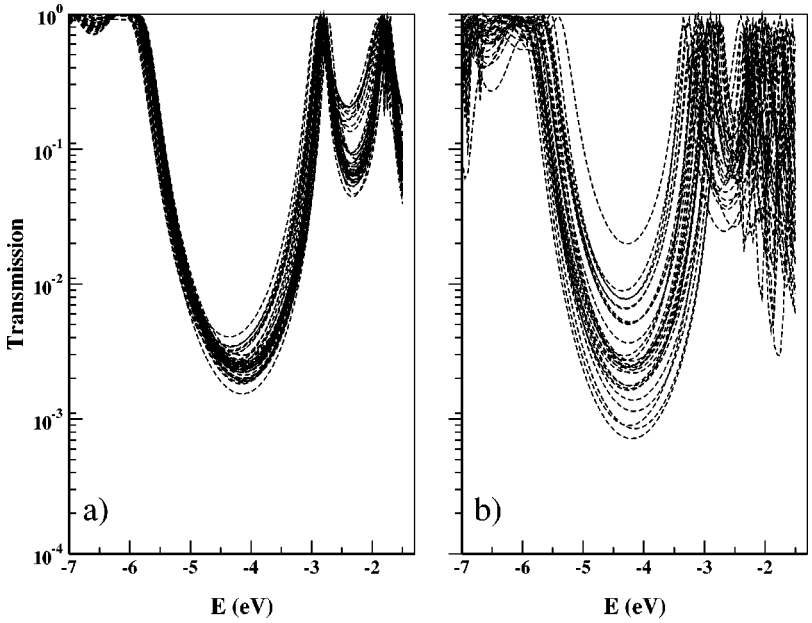

FIG. 3. A family of transmission functions obtained at $T=50$ K for different atomic configurations taken from (a) different times of the MD simulations and (b) different samples of the quantum MC.

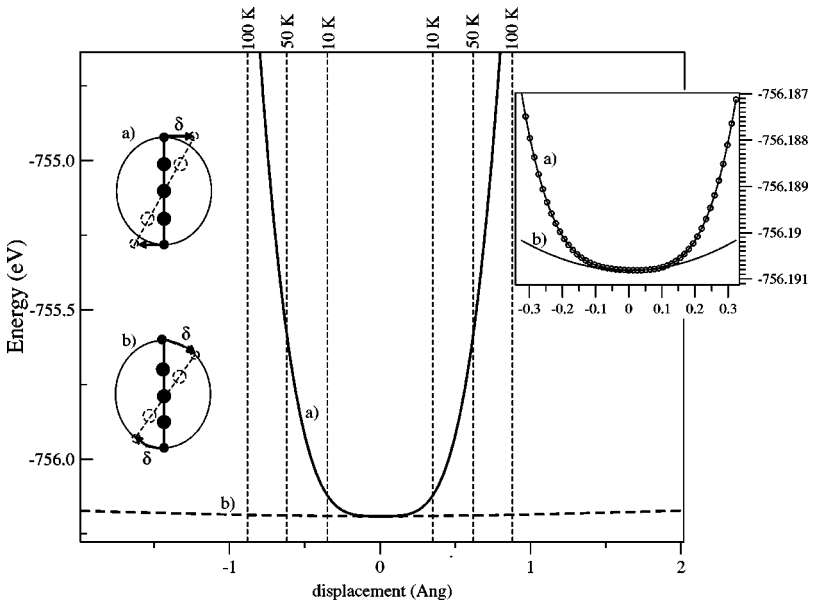

FIG. 4. Potential profile for the twist mode in the DPA molecule. The solid line represents the potential displacing the atoms along (a) the eigenmode and (b) the arc of the rotation. The inset is a zoom around equilibrium.

column of graphs in Fig. 5 corresponds to the distribution of elongations over the molecule. As a general trend, the displacements increase with temperature and decrease as the frequency increases, compare Eq. (2).

The first two modes, which correspond to the first harmonics of a stringlike vibration, can easily be recognized since they have the largest displacements for the atoms closer to the center of the molecule. The maximum displacement in the third mode, which corresponds to the phenyl twist, occurs for the hydrogen atoms while the central carbons do not move. For the lowest modes the deformations can reach values of up to 0.6 Å at 100 K and up to 1.2 Å at room temperature. With such large amplitudes the simple decomposition into normal modes in Eq. (4) does not give correct results. For example, for the third mode, a large oscillation amplitude will not just correspond to a rotation, but it will include a considerable distortion of the phenyl rings and the C-H bonds. A similar effect appears in the first and the second mode before decreasing for the higher modes. The large distortion introduced by the first modes has a great

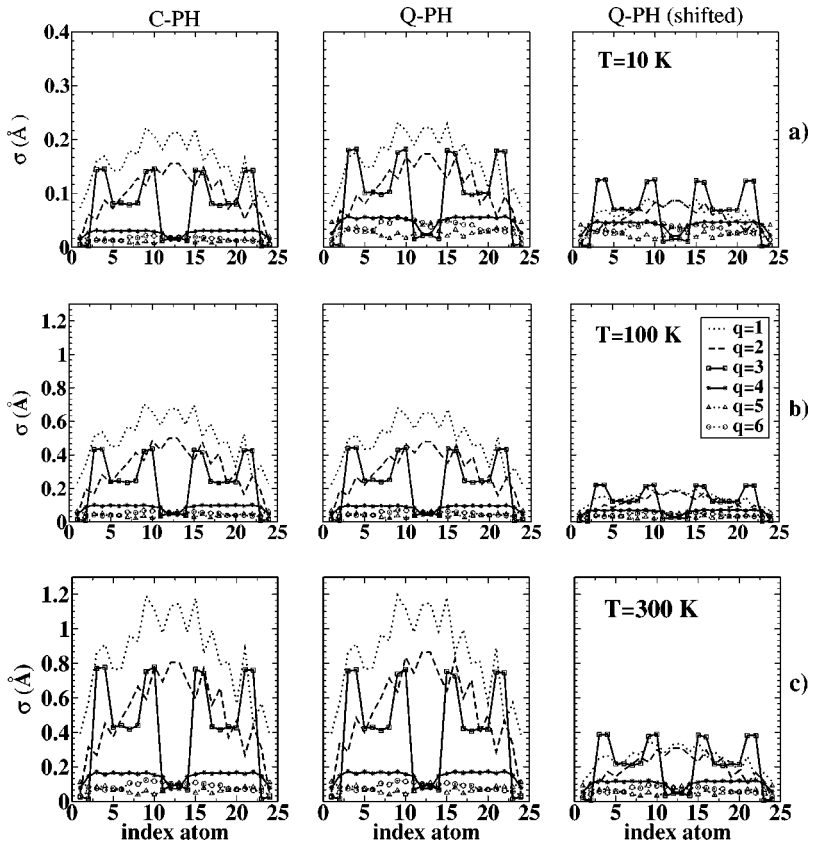

FIG. 5. Oscillation amplitudes for the first six normal modes of vibration resolved for each atom for (a) $T=10$ K, (b) $T=100$ K, and (c) $T=300$ K. The first column refers to classical amplitudes, the second to quantum oscillators, and the third to quantum oscillator with frequency shifted by 20 cm^{-1}. The atom numbers refer to Fig. 1.

effect on the energy spectrum and, as a consequence, on the transmission. In order to account correctly for these nonlinearities within the quantum-mechanical framework, it would be necessary to introduce higher-order expansions of the potential resulting in complex phonon-phonon interactions.

The transition from the low- to the high-temperature regime of the oscillation amplitudes can be emphasized as follows. We have performed a Monte Carlo integration of Eq. (11) in a manner similar to the one described above, but using a classical distribution for the energy of the modes. Equation (3) has been replaced by $E_{th}=kT$, which corresponds to a classical treatment of the oscillators. The results of these computations are shown in Fig. 2(c). This procedure eliminates the zero-point fluctuations and, as an expected consequence, the transmission function at $T=10$ K is essentially the same to the one obtained with the classical MD simulation. However, within this approach the molecular oscillations are treated in the same way as in the quantum treatment. As a consequence $T(E)$ converges to the quantum computations in the limit of high temperatures (compare Figs. 2(b) and 2(c) for $T>200$ K). This is expected, since for $kT \gg \hbar\omega$ the expression of the thermal energy, as given by Eq. (3), converges to kT. Therefore, the vibrational amplitudes of the lowest modes obtained from the quantum and the classical distributions coincide, as can be seen when comparing the first with the second column of Fig. 5. Several observations must be made in order to distinguish the role of the zero-point fluctuations from the influence of the large oscillation amplitudes at high T. First, the elongation of the low-frequency modes is quite similar for the classical and the quantum-mechanical treatment because the mode frequencies are close to the thermal energy at $T=10$ K. This happens because at $T=10$ K, $kT \sim \hbar\omega$ for the lowest modes. However, for the higher modes, the standard deviations decrease much slower in the quantum treatment because of the zero-point energy. An inspection of Eqs. (2) and (3) reveals that in the quantum-mechanical treatment the standard deviation behaves as $\sigma \sim 1/\sqrt{\omega}$ for $\hbar\omega \gg kT$, whereas in the classical approximation $\sigma \sim 1/\omega$ for $\hbar\omega \gg kT$. We conclude that at low temperatures the zero-point fluctuations of all the modes contribute to the average transmission. This can be verified by repeating the computations including the contribution of more internal modes, resulting in larger fluctuations of the transmission. On the contrary, at $T \sim 300$ K the zero-point fluctuations of the nonactivated modes (in this case for $\omega \gtrsim 1300$ cm^{-1}) are dominated by the large oscillation amplitudes of the first few modes. This was also verified by eliminating all but the first six modes, resulting essentially in the same average transmission at $T=300$ K.

Another instructive comparison can be obtained by repeating the quantum MC computations with all the mode frequencies shifted up by a certain amount. This is useful for evaluating the possible systematic errors introduced by the uncertainty on the lowest frequencies inherent in the mode computation, as discussed above. We have chosen a value of 20 cm^{-1} that can be considered as an upper limit for the uncertainty of the frequencies. Obviously, introducing a constant shift to all the frequencies has a larger impact on the oscillation amplitudes of the lowest modes, as visualized in the right column of Fig. 5.

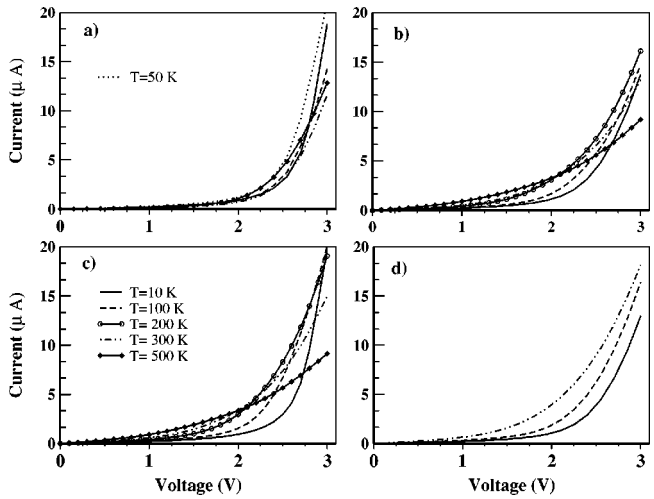

FIG. 6. *I-V* characteristics for the DTT molecule. Results from (a) the MD simulations; (b) the MC with quantum oscillators; (c) the MC with classical oscillators; and (d) the MC with quantum oscillators with frequencies shifted by 20 cm^{-1}.

The results of these computations are shown in Fig. 2(d). At low temperatures the transmission coincides with the previous computations [Fig. 2(b)], since in this regime the zero-point fluctuations of all the modes are so important that the frequency shift does not have major influence. However, at high T, the frequency shift decreases the oscillation amplitudes of the first modes significantly (see Fig. 5). As a consequence, the transmission is not affected by the temperature as much as before since the HOMO and LUMO features survive up to 500 K [compare Fig. 2(d) with Fig. 2(b)]. We conclude that at low temperatures the spectral transmission which includes the elastic scattering due to the quantum fluctuations of the molecule is not strongly affected by errors in the determination of the modes and the associated frequencies. As the temperature increases a realistic representation of the vibrational frequencies becomes more important. However, above a certain critical temperature, which in this case is around 100 K, the anharmonic and nonlinear effects may start to play a critical role which, in any case, the quantum ensemble relying on the harmonic approximation cannot reproduce. Above this temperature, the nonlinear effects are well described within the classical MD approach.

C. *I-V* characteristics

Figure 6 reports the *I-V* characteristics computed from the spectral transmission. The *I-V* curves are obtained by including the bias effect on the Fermi functions in Eq. (9). The Fermi energy of the left electrode is shifted upwards by a quantity $eV/2$ and, correspondingly, the Fermi energy of the right electrode is shifted downwards by $-eV/2$. This is consistent with the approximation that the molecular spectrum shifts almost rigidly by a quantity $eV/2$ when a bias V is applied to the system. A much more time consuming computation would be needed for an accurate computation of the

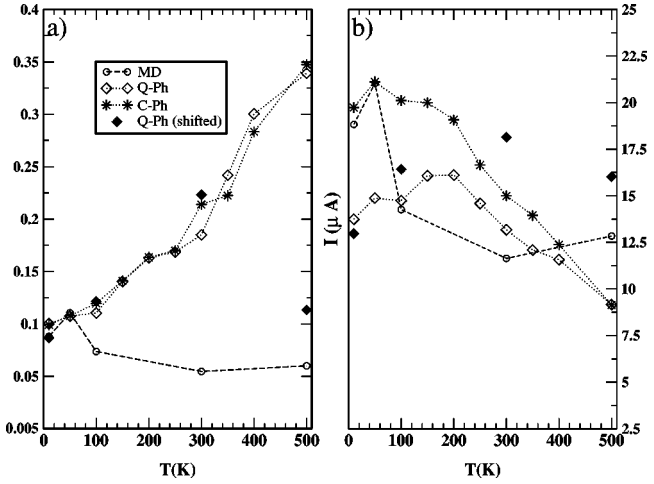

FIG. 7. Current as a function of temperature for the different computational methods for MD, quantum, and classical oscillators. (a) Values obtained at bias=0.5 V and (b) at bias=3.0 V. In both cases the classical oscillator tends to the MD simulations at low T and converges to the quantum treatment at high T.

transmission that is self-consistent with the applied bias, however, the main physical ingredients are already included in this simplified treatment. Moreover, the Fermi function for the charge carriers introduces a further broadening mechanism, but its influence on the current is much smaller with respect to the thermal fluctuations of the molecular geometry.

In the I-V characteristics reported in Fig. 6, the current at low biases increases and at high biases decreases, a direct consequence of the gap fluctuations. This effect is more pronounced in the quantum computations than in the MD simulations. The trend is summarized in Fig. 7, which shows the current as a function of temperature at the voltages of 0.5 V and 3.0 V. Both in the low- and the high-voltage regime the MD current approaches the classical MC result and around 50 K both give similar results. Note that the MD and classical MC results do not coincide at 10 K due to deviations from the harmonic approximation affecting the lowest vibrational modes already in this temperature regime, compare Fig. 4. As the temperature rises, both computational schemes give different results, particularly at low voltages, where the gap tunneling dominates. According to the MD simulations, above 200 K there are no significant current variations because the important modes which affect the transport are all activated.

At low T and high voltages, the quantum computation gives significantly different results from the classical approaches because the resonant tunneling contributes significantly. However, at high temperature the classical and quantum MC sampling give similar results over the entire voltage range.

A subject of current investigation is the effect of inelastic scattering on the molecular electric conduction.[37] However, based on the results shown in the present work, the inelastic scattering in the high-temperature regime is a challenging problem because it requires the inclusion of anharmonic effects. Moreover, at room temperature the phonon population of the low-frequency modes is so large that multiple scattering events may become important.

It should also be observed that the usual experimental configuration employed to measure the conductance of such molecules is in self-assembled monolayers (SAM's). In such conditions, the interactions between neighboring molecules and collective oscillations can also play an important role in the determination of the energetically more stable configuration and the vibrational frequencies of the lowest modes.[38]

TABLE III. Vibrational frequencies for the DDP molecule.

Mode	Frequency (cm^{-1})
1	12.89
2	16.18
3	19.79
4	31.59
5	42.83
6	59.22
7	75.80
8	81.18
9	86.40
10	104.52
⋮	⋮
94	3059.11
95	3688.55
96	3692.79

D. Thermal effects on a DDP molecule

For comparisons with the simple DTT, we have also investigated the influence of thermal fluctuations on the transport through a DDP molecule [Fig. 1(b)]. This molecule is in the class of the Aviram-Ratner[39] molecular diodes and was also proposed by Ellenbogen[40] as a prototype of a rectifying device. The molecule consists of two benzene rings linked together by a barrier bridge (an alkyl chain). The two parts are chemically modified in order to act as electron donor or acceptor, resulting in electronic orbitals localized either on the donor or the acceptor side when no bias is applied. Under bias the rectification mechanism is governed by the asymmetry in the level alignment. Under forward bias, the energy levels of the donor and the acceptor can be aligned with the Fermi level of the emitter, resulting in an enhancement of the resonant tunneling.

In the case discussed here the CN groups act as electron donors and raise the energy levels of the phenyl ring, whereas the OH groups act as electron acceptors and lower the levels. Concerning the mode frequencies reported in Table III, the lowest modes are, again, associated with the lowest harmonics of stringlike vibrations. The highest frequencies shown correspond to the C-H stretching and the O-H stretching (about 3690 cm^{-1}).

Figure 8 shows the calculated I-V characteristics obtained from classical MD simulations and the quantum MC sampling. The findings are qualitatively similar to those of the TTP molecule.

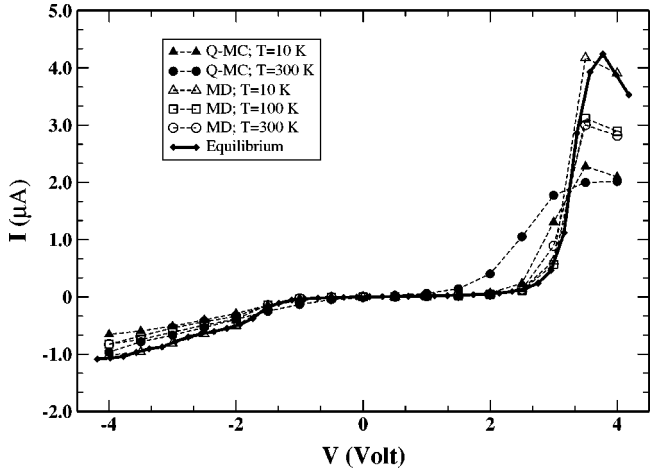

FIG. 8. *I-V* characteristics for the DDP molecule for different temperatures obtained from the MD simulations and the quantum treatment of the oscillators.

Higher temperatures reduce the current and lower the rectification ratio. This effect is stronger in the case of the quantum MC simulations, for reasons similar to those presented for the TTP molecule. Also in this case the Bose-Einstein ensemble gives the correct low-temperature limit where the transport is influenced by the zero-point motion of all internal modes. As a result the peak current given by the quantum MC calculation at 10 K is only half of the current obtained for the equilibrium configuration. At high temperatures the harmonic approximation is no more applicable, giving a strong broadening of the *I-V* curve.

Just as in the case of the TTP molecule the MD simulations saturate above 200 K, so that the *I-V* curve does not show a significant temperature dependence.

E. Frequency analysis of the time-dependent current

The MD simulations allow the investigation of the time dependence of the tunneling current, revealing signatures of the vibrational modes.

In order to show the relationship between the time-dependent signal and the vibrational eigenmodes, we have reported in Figs. 9 and 10 the Fourier spectrum of the time-dependent current through a DTT molecule together with the vibrational frequencies. Figure 9 shows the time-resolved current and corresponding Fourier spectrum for a temperature of 10 K and a bias voltage of 1 V. Figure 10 reports a similar calculation for a temperature of 300 K. The time evolution confirms the consistency with the vibrational modes. Indeed, several peaks exactly correspond to specific modes, especially above 300 cm^{-1}. In general, the modes which affect most strongly the tunneling current are characterized by stretching motion of the central carbon bridge, by a skewing motion of the phenyl rings influencing the C-S bond, and by S-Au stretching.

The strongest peaks coincide with the vibrational modes that give the largest perturbation to the current. Beginning from the highest frequencies, the stretching of the central C-C triple bond at 2400 cm^{-1} has a large impact on the transmitted current. This large effect is intuitively obvious considering that the current flows entirely along this bond. The *z* deformation of the phenyl rings, which leaves the central bridge and the sulfur atoms frozen, also has a large effect as revealed by the peak at the frequency of 1798 cm^{-1}. Further down the influence of the phenyl breathing mode is also strong, at the frequency of 1272 cm^{-1}. The *z* stretching of the rings, with consequent change in distance of the C-S and the central C-C bridge, occurs in correspondence of the peaks at 1170 and 1153 cm^{-1}. At 521 cm^{-1} corresponds the almost rigid Ph-S oscillation along the *z* axis. Very strong is the effect of the modes around 400 cm^{-1} which involves the S-Au bond stretching. The lowest part of the frequency spectrum tends to be quite noisy. This is dominated by the phenyl twist mode, which is labeled as mode 3 in Table II. This mode is appreciably softened as a signature of nonharmonic effects which intervene already at 10 K. The strongest peak is actually located at twice the frequency of the twist mode (around 31 cm^{-1}). This doubling effect comes simply from

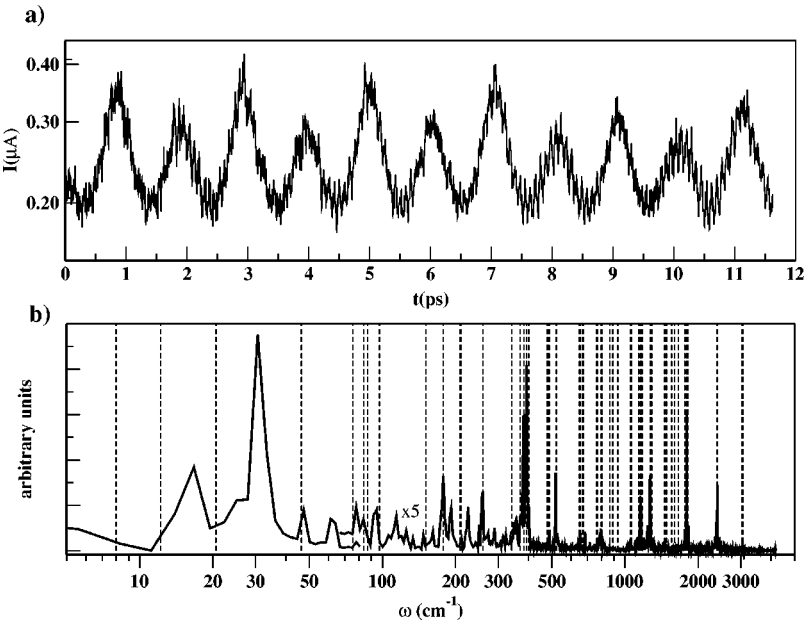

FIG. 9. (a) MD simulation of the time-dependent current for the DTT molecule at $T = 10$ K. (b) Frequency spectrum analysis of the current compared to the frequencies of the vibrational modes (dashed lines). The spectrum is magnified by a factor of 5 above 70 cm^{-1}.

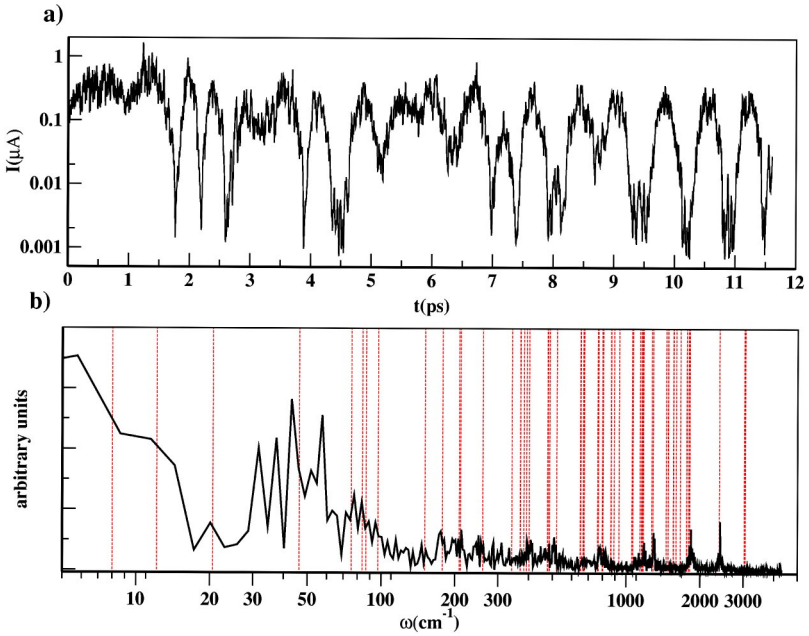

FIG. 10. (a) MD simulation of the time-dependent current for the DTT molecule at $T = 300$ K. (b) Frequency spectrum analysis of the current compared to the frequencies of the vibrational modes (dashed lines).

the specular symmetry of the transmission between the configurations occurring every half period of oscillation of such mode.

Sum frequencies and other complex nonlinear behaviors are all present but much more difficult to distinguish. Satellite peaks, with frequency sum and subtraction of the important low-frequency mode of 15 cm^{-1}, appear clearly around the modes at 151, 178, and 211 cm^{-1}. A large number of satellite peaks which clearly originate from frequency summation and subtractions appear around all the main peaks above 300 cm^{-1}.

At the temperature of 300 K the low-frequency spectrum is completely broadened by nonlinearities. The molecules freely rotate and each rotation can be well recognized in the time-dependent signal as a strong decrease of current. In the higher part of the spectrum a number of modes present at 10 K still survive, although broadened.

This information is very difficult to explore experimentally, since it would require ultrafast response measurements. Furthermore, the current signal and the resulting noise is extremely small. Amplifications of such noises are possible from the transmission through a large number of molecules (e.g., on a SAM) with alternating currents.

According to Ref. 37 the largest contribution to the inelastic scattering should be expected from the modes which maximize the variation of the transmission amplitude, i.e., exactly from those modes which present a high peak in the frequency spectrum discussed here. According to Ref. 10, for gap transmission, the inelastic component of the current is expected to be one to two orders of magnitude smaller than the elastic. Only at high bias voltage, when the resonant tunneling plays a dominant role, the inelastic component should compete with the elastic one.

Despite a number of difficulties, frequencies up to 50–100 GHz can be reached experimentally, therefore the lowest frequency of 1 GHz, corresponding to the phenyl twist, may accessible. The behavior of the metal contacts and the tunneling currents at such high frequencies has been studied very little,[41] however, we can expect that the resonant responses to high-frequency signals could provide the access to the vibrational spectrum of organic molecules and give the possibility to study a number of phenomena such as surface aggregation and collective motions.

IV. CONCLUSIONS

We have computed the effect of coherent phonon vibrations on the transmission through molecular wires. The computations have been performed using MD simulations which treat the molecular vibrations classically. These computations have been compared with averages over the ensemble of the configurations obtained from a quantum-mechanical treatment of the mode oscillators. These treatments start from the determination of the normal modes of vibrations obtained from the diagonalization of the Hessian. To each mode is then associated a quantum-mechanical distribution probability which in thermal equilibrium depends on the number of excited quanta in the mode. The molecular configuration is found from the product of the independent mode distributions and the average over the configuration space is obtained by means of a Monte Carlo integration. The computations reveal that the harmonic approximation looses validity as the temperature increases and the simple first-order expansion of the atomic displacements into normal modes of vibrations give inaccurate results already at 100 K. On the other hand, the molecular dynamics, although classical, gives a more correct treatment of the molecular vibrations at high temperatures, since it treats more accurately nonlinear behaviors which occur when the oscillations become large. At low temperatures the quantum-mechanical treatment takes into account the zero-point motion of the oscillators, which is completely missed in the classical approximations. The harmonic approximation is sufficiently accurate for these molecules at 10 K. Increasing the temperature we found a de-

crease in the HOMO-LUMO gap energy.

We have also shown that the time-resolved current obtained with the MD simulations is consistent with the frequency spectrum. The method provides a relatively simple overview on which modes have the largest effects on the transport properties.

ACKNOWLEDGMENTS

The work was supported by the European project DIODE. EU funded Human Potential Research Training Network (Contract No. HPRN-CT-1999-00164).

[1] J. Chen, M.A. Reed, A.M. Rawlett, and J.M. Tour, Science **286**, 1550 (1999).
[2] J.M. Seminario, A.G. Zacarias, and J.M. Tour, J. Am. Chem. Soc. **122**, 3015 (2000).
[3] M.A. Reed, J. Chen, A.M. Rawlett, D.W. Price, and J.M. Tour, Appl. Phys. Lett. **78**, 3735 (2001).
[4] X.D. Cui, A. Primak, X. Zarate, J. Tomfohr, O.F. Sankey, A.L. Moore, T.A. Moore, D. Gust, G. Harris, and S.M. Lindsay, Science **294**, 571 (2001).
[5] S.T. Pantelides, M. Di Ventra, N.D. Lang, and S.N. Rashkeev, IEEE Trans. Nanotech. **1**, 86 (2002).
[6] C. Zhou, M.R. Deshpande, M.A. Reed, L. Jones, and J.M. Tour, Appl. Phys. Lett. **71**, 611 (1997).
[7] R.M. Metzger, B. Chen, U. Hopfner, M.V. Lakshmikantham, D. Vuillaume, T. Kawai, X.L. Wu, H. Tachibana, T.V. Hughes, H. Sakurai, J.W. Baldwin, C. Hosch, M.P. Cava, L. Brehmer, and G.J. Ashwell, J. Am. Chem. Soc. **119**, 10455 (1997).
[8] B.C. Stipe, Curr. Opin. Solid State Mater. Sci. **4**, 421 (1999).
[9] J.L. D'Amato and H.M. Pastawski, Phys. Rev. B **41**, 7411 (1990).
[10] H. Ness, S.A. Shevlin, and A.J. Fisher, Phys. Rev. B **63**, 125422 (2001).
[11] K. Stokbro, B. Yu-Kuang Hu, C. Thirstrup, and X.C. Xie, Phys. Rev. B **58**, 8038 (1998).
[12] N. Lorente and M. Persson, Phys. Rev. Lett. **85**, 2997 (2000).
[13] N. Mingo and K. Makoshi, Phys. Rev. Lett. **84**, 3694 (2000).
[14] J. Bonca and S.A. Trugman, Phys. Rev. Lett. **75**, 2566 (1995).
[15] K. Haule and J. Bonca, Phys. Rev. B **59**, 13087 (1999).
[16] L.E.F. Foa Torres, H.M. Pastawski, and S.S. Makler, Phys. Rev. B **64**, 193304 (2001).
[17] E.G. Emberly and G. Kirczenow, Phys. Rev. B **61**, 5740 (2000).
[18] R.P. Feynman, *Statistical Mechanics: A Set of Lectures* (Perseus, Cambridge, MA, 1998), ISBN 0201360764.
[19] M. Elstner, D. Porezag, G. Jungnickel, J. Elsner, M. Haugk, Th. Frauenheim, S. Suhai, and G. Seifert, Phys. Rev. B **58**, 7260 (1998).
[20] D. Porezag, Th. Frauenheim, Th. Köhler, G. Seifert, and R. Kaschner, Phys. Rev. B **51**, 12947 (1995).
[21] V. Mujica, M. Kemp, and M.A. Ratner, J. Chem. Phys. **101**, 6849 (1994).
[22] A. Di Carlo, P. Vogl, and W. Pötz, Phys. Rev. B **50**, 8358 (1994).
[23] S. Datta, Superlattices Microstruct. **28**, 253 (2000).
[24] S. Datta, *Electronic Transport in Mesoscopic System* (Cambridge University Press, Cambridge, 1995), Chap. 3.
[25] A. Di Carlo, M. Gheorghe, P. Lugli, M. Stenberg, G. Seifert, and Th. Frauenheim, Physica B **314**, 86 (2002).
[26] F. Guinea, C. Tejedor, F. Flores, and E. Louis, Phys. Rev. B **28**, 4397 (1983).
[27] T.N. Todorov, J. Phys.: Condens. Matter **14**, 3049 (2002).
[28] Y. Yourdshahyan, H.K. Zhang, and A.M. Rappe, Phys. Rev. B **63**, 081405(R) (2001); A. Johansson and S. Stafström, Chem. Phys. Lett. **322**, 301 (2000).
[29] P. Markos and B. Kramer, Ann. Phys. (Leipzig) **2**, 339 (1993).
[30] P.D. Kirkman and J.B. Pendry, J. Phys. C **17**, 4327 (1982); **17**, 5707 (1984).
[31] M. Verlet, Phys. Rev. **159**, 98 (1967).
[32] G. Seifert and R. Schmidt, New J. Chem. **16**, 1145 (1992).
[33] J.M. Seminario and P.A. Derosa, J. Am. Chem. Soc. **123**, 12418 (2001).
[34] Z. Chernia, T. Livneh, I. Pri-Bar, and J.E. Koresh, Vib. Spectrosc. **25**, 119 (2001).
[35] R. Scholz, A.Yu. Kobitski, T.U. Kampen, M. Schreiber, D.R.T. Zahn, G. Jungnickel, J. Elsner, M. Sternberg, and Th. Frauenheim, Phys. Rev. B **61**, 13 659 (2000).
[36] A.Yu. Kobiski, R. Scholz, and D.R.T. Zahn, J. Mol. Struct.: THEOCHEM **625**, 39 (2003).
[37] A. Troisi and M.A. Ratner, J. Chem. Phys. **118**, 6072 (2003).
[38] J.M. Seminario, A.G. Zacarias, and J.M. Tour, J. Am. Chem. Soc. **120**, 3970 (1998).
[39] A. Aviram and M.A. Ratner, Chem. Phys. Lett. **29**, 277 (1974).
[40] J.C. Ellenbogen and J.C. Love, Proc. IEEE **88**, 386 (2000).
[41] R. Baer and D. Neuhauser, Int. J. Quantum Chem. **91**, 524 (2003).